Published OnlineFirst March 9, 2010; DOI: 10.1158/0008-5472.CAN-09-2408
Published Online First on March 9, 2010 as 10.1158/0008-5472.CAN-09-2408

Cancer Research

Oncolytic Viral Therapy for Prostate Cancer: Efficacy of Reovirus as a Biological Therapeutic

Chandini M. Thirukkumaran[1,5], Michael J. Nodwell[9], Kensuke Hirasawa[10], Zhong-Qiao Shi[5], Roman Diaz[5], Joanne Luider[7], Randal N. Johnston[1,2], Peter A. Forsyth[1,5], Anthony M. Magliocco[1,3,5,7], Patrick Lee[11], Sandra Nishikawa[2], Bryan Donnelly[4], Matt Coffey[8], Kiril Trpkov[3,7], Kevin Fonseca[6], Jason Spurrell[5], and Don G. Morris[1,5]

Abstract

Reovirus is a nonattenuated double-stranded RNA virus that exploits aberrant signaling pathways allowing selective cytotoxicity against multiple cancer histologies. The use of reovirus as a potential treatment modality for prostate cancer has not previously been described, and in this study evidence of *in vitro* and *in vivo* activity against prostate cancer was seen both in preclinical models and in six patients. The human prostate carcinoma cell lines PC-3, LN-CaP, and DU-145 exposed to replication-competent reovirus showed evidence of infection as illustrated by viral protein synthesis, cytopathic effect, and release of viral progeny. This oncolytic effect was found to be manifested through apoptosis, as DNA fragmentation, Apo 2.7 expression, Annexin V binding, and poly(ADP-ribose) polymerase cleavage were observed in live reovirus-infected cells, but not in uninfected or dead virus–treated cells. *In vivo*, hind flank severe combined immunodeficient/nonobese diabetic murine xenograft showed reduction in tumor size when treated with even a single intratumoral injection of reovirus. Finally, intralesional reovirus injections into a cohort of six patients with clinically organ-confined prostate cancer resulted in minimal side effects and evidence of antitumor activity. Histologic analysis after prostatectomy found a significant CD8 T-cell infiltration within the reovirus-injected areas as well as evidence of increased caspase-3 activity. These findings suggest that reovirus therapy may provide a promising novel treatment for prostate cancer and also imply a possible role for viral immune targeting of tumor. *Cancer Res; 70(6); 2435–44. ©2010 AACR.*

Introduction

Metastatic prostate carcinoma is the second leading cause of cancer-related deaths in North American males (1). In 2009, it is estimated that >185,000 new cases and 28,500 deaths will result from this disease in the United States (1). Globally, prostate cancer accounts for >220,000 deaths annually (2). Current therapeutic options for advanced prostate cancer are limited to androgen deprivation and/or cytotoxic chemotherapy with the goals of treatment to extend survival while maintaining quality of life. Clearly more efficacious and/or novel treatments are required.

Authors' Affiliations: Departments of [1]Oncology, [2]Medical Biochemistry, [3]Pathology, and [4]Urology, University of Calgary; [5]Tom Baker Cancer Center; [6]Provincial Laboratory for Public Health; [7]Calgary Laboratory Services; [8]Oncolytics Biotech Inc., Calgary, Alberta, Canada; [9]Bio-Rad Laboratories (Canada) Ltd., Mississauga, Ontario, Canada; [10]Memorial University of Newfoundland, St John's, Newfoundland, Canada; [11]Department of Microbiology and Immunology, Dalhousie University, Halifax, Nova Scotia, Canada

Note: Primary authorship is shared by C.M. Thirukkumaran, M.J. Nodwell, and K. Hirasawa.

Corresponding Author: Don G. Morris, Department of Oncology, Tom Baker Cancer Centre, 1331, 29 Street NW, Calgary, Alberta, Canada T2N 4N2. Phone: 403-521-3437; Fax: 403-283-1651; E-mail: donmorri@cancerboard.ab.ca.

doi: 10.1158/0008-5472.CAN-09-2408

Over the past decade both naturally occurring and genetically modified oncolytic viruses have been investigated as a potential treatment for a myriad of cancers. One such virus, reovirus (respiratory, enteric, orphan), is a common nonattenuated environmental double-stranded RNA virus that has been shown to have oncolytic potential against many cancers, including lymphoid, colon, ovarian, breast, pancreatic, and high-grade glioma cancer cell lines, as well as their *ex vivo* correlates (3–7). Moreover, only mild symptoms are experienced by healthy adults during infection due to its tropism for transformed cells with aberrant signaling pathways (8–10). The underlying mechanism(s) behind the preferential cytotoxicity of reovirus toward transformed cells has only recently been described and seems to be at the level of intracellular signaling and not at cell surface attachment (11). When reovirus-resistant murine NIH 3T3 cells are transformed with oncogenes, such as *v-erb*B_2, *sos*, and *ras*, reovirus susceptibility is conferred (9–11). Reovirus likely exploits an activated Ras/oncogenic signaling pathway, taking advantage of the inhibition of the double-stranded RNA–activated protein kinase found in these cells (11). Recent data has implicated the Ras/RalGEF/p38 pathway in an NIH 3T3 model system of reovirus oncolysis (12).

Although the initial malignant transformation of prostate epithelial cells is not generally felt to be a *ras* mutation–dependent event, there are several other pathways felt to be important in both malignant transformation and involved

Published OnlineFirst March 9, 2010; DOI: 10.1158/0008-5472.CAN-09-2408

in progression to advanced hormone-resistant disease that may involve the Ras pathway. Recent studies involving *in vivo* prostate mouse models and patient tissue specimens indicate a link between the PTEN/phosphoinositide 3-kinase/AKT signaling pathway involving mTOR and the mitogen-activated protein kinase cascade (Ras/Raf/MEK/ERK; refs. 13, 14). This progressive cross-talk between complex signaling pathways may lead to the cellular susceptibility to reovirus of prostate cancer.

Many oncolytic viruses including reovirus exert their activity by triggering apoptotic pathways (15, 16). The specific apoptotic pathways for reovirus oncolysis in prostate cancer are currently undefined and seem to be different depending on the histologic origin of the susceptible cell. Studies have shown that reovirus infection induces apoptosis in cultured cancer cells *in vitro* (17, 18) in a p53-independent mechanism that involves cellular proteases, including calpains and caspases (19, 20). In turn, this process has been shown to be dependent on NF-κB activation (21, 22) and is inhibited by overexpression of Bcl-2 (17). It has also been shown that the binding of tumor necrosis factor–related ligand (TRAIL) to its cellular receptors TRAIL R2 and TRAIL R1 mediates reovirus-induced apoptosis involving caspase-8 in both HeLa and HEK293 cells (23).

The current studies were performed to determine the efficacy of reovirus as an experimental therapeutic for prostate cancer *in vitro* and *in vivo* in a murine model. In addition, the specific mechanism of virus-mediated cell death was identified and reovirus efficacy in a cohort of six prostate cancer patients was confirmed. This is the first study to show the use of reovirus as an anticancer therapeutic against prostate cancer under preclinical and clinical settings.

Materials and Methods

Cell Lines

All established cell lines were obtained from the American Type Culture Collection, except for PrEC cells (Lonza Walkersville, Inc.). All cancer cells were grown in media containing 10% fetal bovine serum (FBS). PC-3 cells were cultured in RPMI 1640 supplemented with sodium glutamate [Life Technologies Bethesda Research Laboratories (BRL)]. DU-145, L929, and MCF-7 cells were cultured in DMEM supplemented with sodium pyruvate (Life Technologies BRL). LN-CaP cells were cultured in RPMI 1640 containing 1 mmol/L HEPES buffer plus sodium pyruvate (Life Technologies BRL), and PrEC cells were maintained in PrEGM medium. Each cell line was tested to exclude *Mycoplasma* contamination.

Reovirus

Reovirus serotype 3 (Dearing strain) was grown in L-929 suspensions and purified as previously described (24), except that β-mercaptoethanol was omitted from the extraction buffer. Reovirus was inactivated via short wavelength UV exposure for 30 min in a six-well plate. UV-inactivated reovirus (dead reovirus, DV) was then checked for activity and sterility by plating onto susceptible L-929 cell monolayers and culturing for up to 1 wk. Viral titers were obtained from L-929 cells using the plaque titration method as previously described (19).

Immunofluorescent Analysis of Reovirus Infection

Cells at 60% confluency were infected with either live reovirus (LV) or DV at a multiplicity of infection (MOI) of 40 plaque-forming units (pfu) per cell. At 2, 24, and 48 h postinfection, cells were trypsinized and intracellular staining was performed following permiabilization of cell membranes (IntraPrep Permeabilization Reagent, Beckman-Coulter), followed by primary antibody (rabbit polyclonal antireovirus type 3 serum, a kind gift from Dr. P.W.K. Lee, 1:20) and secondary antibody (goat anti-rabbit IgG FITC conjugate, DAKO, 1:100) staining. Immunofluorescent cells were photographed under a UV microscope (NikonY-THS).

Radiolabeling of Reovirus-Infected Cells, Immunoprecipitation of Reovirus Proteins, and SDS-PAGE

Subconfluent monolayers of cell lines were infected with reovirus at a MOI of 40 pfu per cell. At 0, 24, and 48 h postinfection, the medium was replaced with DMEM containing 10% dialyzed FBS and 0.1 μCi/mL of [^{35}S]methionine. After further incubation for 12 h at 37°C, the cells were washed in PBS and lysed in PBS containing 1% Triton X-100, 0.5% sodium deoxycholate, and 1 mmol/L EDTA. Nuclei and cell membrane debris were then removed by centrifugation at 450 × *g*, and the supernatants were stored at −80°C. To reduce nonspecific background, immunoprecipitation of [^{35}S]-labeled reovirus-infected cell lysates with polyclonal antireovirus antibody was performed as described previously (5). Whole-cell, as well as immunoprecipitated, extracts were subjected to SDS-PAGE and subsequent autoradiography.

Viral Progeny Production

Prostate cancer cells were grown in 12-well plates and infected with 40 MOI of reovirus. To evaluate virus progeny production, the cells were frozen at −80°C at 0, 12, 24, 36, 48, 60, and 72 h postinfection. The frozen plates were subjected to three freeze/thaw cycles, and supernatants were plaque titrated on L929 cells. Three independent experiments were performed per cell line.

Animals

Five- to eight-week-old male severe combined immunodeficient (SCID)/nonobese diabetic (NOD) mice were purchased from the Cross Cancer Institute. The animals were housed in a sterile animal facility with food and water *ad libitum*. All procedures were reviewed and approved by the University of Calgary Animal Care Committee.

In vivo Studies in a s.c. Xenograft Model

Subconfluent cells growing in exponential phase were harvested, washed, and resuspended in sterile PBS at a density of 2×10^7 cells/mL. SCID/NOD mice were injected s.c. with 2.0×10^6 cells suspended in 100 μL of PBS in the hind flank. For LN-CaP, 2.0×10^6 cells suspended in 50 μL of

Published OnlineFirst March 9, 2010; DOI: 10.1158/0008-5472.CAN-09-2408

Matrigel diluted 1:1 in PBS (Collaborative Biomedical Products) were injected. After 2 to 3 wk, mice with palpable tumors measuring ~0.25 cm^2 received a single intratumoral injection of 1.0×10^7 pfu of either live or UV-inactivated reovirus in 20 μL sterile PBS. Tumor size was measured and recorded twice weekly. Mice were sacrificed when they lost 25% body weight and/or had problems with ambulating, feeding, or grooming.

Apoptotic Assays

The prostate cancer cell lines were infected with either no virus, 40 MOI of DV, or 40 MOI of LV. Following viral absorption at 4°C for 45 min, the plates were incubated for 24, 48, 72, and 96 h and cells were harvested following trypsinization and centrifugation. Cell pellets were then washed in PBS twice before subsequent staining as per manufacturer's instructions and flow cytometric analysis.

DNA fragmentation. Cell pellets were resuspended in 1 mL of 50 μg/mL of propidium iodide (PI)/RNAase/Triton X-100 (Sigma Chemical Co.). One hundred microliters of Flow Count Beads (Beckman-Coulter) were then added to each tube. After incubating tubes for 15 min, samples were analyzed using a Coulter Epics EL-MCL flow cytometer (Beckman-Coulter). Intact cells were enumerated using Flow Count Beads as an internal calibrator.

Annexin V/7-AAD. Cell pellets were resuspended in 100 μL of Binding Buffer (Molecular Probes Eugene). Annexin V-FITC (5 μL; Molecular Probes) and 7-AAD (20 μL; Molecular Probes) were added. Tubes were pulse-vortexed and incubated for 15 min at room temperature, after which 900 μL of Binding Buffer were added. Flow cytometric analysis was performed with apoptotic cells defined as those being Annexin V positive and 7-AAD negative.

APO 2.7. Cell pellets were resuspended in 100 μL of IntraPrep Reagent 1 (Beckman-Coulter) and incubated at room temperature for 15 min. The washed cells were resuspended in 100 μL of IntraPrep Reagent 2 and 20 μL of APO2.7-PE (Beckman-Coulter) and incubated for an additional 15 min. Cells were washed again in PBS, resuspended in 1 mL of PBS, and analyzed.

Western Blot Analysis of Poly(ADP-Ribose) Polymerase Cleavage

MCF-7 and the three prostate cancer cell lines were cultured with either cisplatin (10 μg/mL), no virus, LV (40 MOI), or DV (40 MOI). At 24 or 48 h, cells were lysed and sonicated in a solution comprising of 0.2% SDS, 1% triton X-100, 5 mmol/L EDTA, 10 μg/mL leupeptin, 10 μg/mL aprotinin, and 10 μg/mL antipain in PBS (Sigma Chemical Co.). Cell extracts comprising 35 μg of protein were separated by SDS/PAGE, electrotransferred to nitrocellulose membranes, and blocked with 5% nonfat milk in PBS-Tween (0.15%) for 1 h. Membranes were incubated overnight (4°C) with anti–poly(ADP-ribose) polymerase (PARP; 1 μg/mL, Oncogene) and horseradish peroxidase (HRP)–conjugated anti-IgG secondary antibody (1:2,000, Oncogene). Bands were visualized with chemoluminescence reagent (New England Biolabs).

Patient Recruitment, Inoculation, and Follow-up

Patients were recruited from our local prostate cancer referral clinics at Rockyview Hospital and Tom Baker Cancer Centre in Calgary, Canada. After Health Canada and the local independent review board approval, patients were asked to sign informed consent and eligibility for the study reviewed. Pathology from the original transrectal ultrasound (TRUS) guided biopsies, imaging that confirmed organ confined disease, patient overall suitability, and agreement for radical prostatectomy were confirmed. Normal hematologic, hepatic, and cardiac function was required, as well as the requirement for patients not to be on any systemic immunosuppression. REOLYSIN (clinical grade reovirus; GMP) was injected

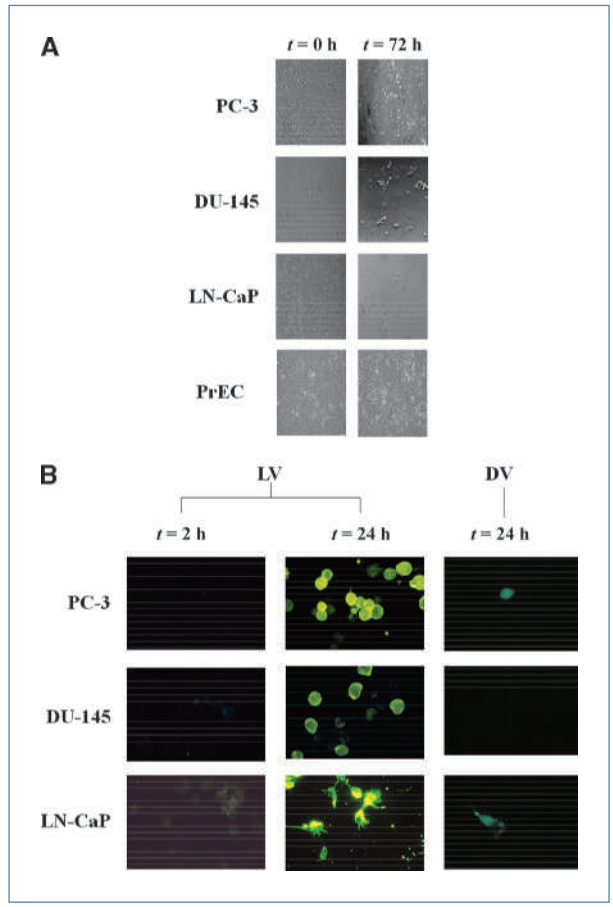

Figure 1. A, cytopathic effect of reovirus on established prostate cancer cell lines and normal prostate epithelial cells. Cell monolayers were infected with LV at a MOI of 40 pfu per cell and photographed at 72 h. Widespread killing was observed in all prostate cancer cell lines, but not in low-passage normal prostate epithelial PrEC cells at 72 h post virus infection. In all cases, dead virus controls were similar to pretreatment cells at 72 h (data not shown). B, immunofluorescence analysis of reovirus infection. Prostate cancer cells were grown to ~40% confluency and infected with LV or DV. At 2 and 24 h postinfection, cells were trypsinized, stained with antireovirus antibody and FITC-conjugated secondary antibody, and photographed (400× magnification). Note the significant increase in viral proteins (fluorescence) at 24 h with LV treatment, but not with DV treatment.

Published OnlineFirst March 9, 2010; DOI: 10.1158/0008-5472.CAN-09-2408

via transrectal ultrasound in 1 mL of PBS into a suitable lesion, and a sterile metal coil was left at the injection site to facilitate localization of the injected lesion at the time of pathologic analysis after prostatectomy. Patients were then followed weekly for 3 weeks for toxicity, evidence of viral shedding, and prostate-specific antigen (PSA) levels before prostatectomy. A reference prostate pathologist reviewed all specimens. Toxicity and adverse events were graded as per the National Cancer Institute Clinical Trials Group (NCI CTG) expanded Common Toxicity Criteria, version 4. Dose-limiting toxicity was defined as grade ≥3 toxicity and felt to be possibly/probably related to the agent/treatment protocol.

Reverse Transcription–PCR and Viral Culture for Detection of Shedding

Urine, stool, and serum from patients at various time points were analyzed for evidence of REOLYSIN by extracting RNA using QiaAmp Viral RNA Minikits (Qiagen). Equal quantities of RNA were transcribed with hexanucleotide primers, and PCR was performed with reovirus s3 cDNA targeted primers: forward, 5′-GGGCTGCACATTACCACTGA-3′ and reverse, 5′-CTCCTCGCAATACAACTCGT-3′. PCR reaction mixture was denatured at 95°C for 3 min and cycled for 35 cycles (95°C for 30 s, 60°C for 30 s, and 72°C for 30 s). Extension was followed at 72°C for 7 min. An expected PCR product of 290 bp was analyzed on 1.5% agarose gels.

Neutralizing Antibody Quantification from Patient Specimens

Analysis of reovirus serotype 3 neutralizing antibodies from patient's sera used a cell-based assay involving the reduction of cytopathic effect on the sensitive indicator L929 cell line. Briefly, L929 cells were plated in triplicate at a density of 10,000 per 96-well plate for 24 h followed by serial dilutions of patient sera incubated with LV or DV at an MOI of 40 for an additional 24 h and analyzed for viability using a WST assay (25).

Immunohistochemistry of Patient Prostate Tumor

Resected patient prostate tumors were fixed in 10% phosphate-buffered formalin and embedded in paraffin. For immunohistochemistry staining, 5-μm thick sections attached to microscope slides were deparaffinized and rehydrated. Antigen retrieval was achieved by steam treatment in high-pH Tris-EDTA buffer (pH 9.0) for 25 min. To quench endogenous peroxidase, these were next treated with 1% hydrogen peroxide in methanol for 10 min.

CD4 and CD8 staining. Diluted primary antibodies (1:30, CD4, Vector Laboratories and 1:100, CD8, DakoCytomation) were applied to sections and incubated at 4°C overnight. They were next processed at room temperature with secondary antibody (1:100, biotinylated horse anti-mouse immunoglobulin, Vector Labs) for 1 h and a further 30-min incubation with ABC Elite reagent containing both avidin and HRP (Vector Labs). Finally the slides were exposed to 3,3′-diaminobenzidine (0.7 mg/mL) and urea hydrogen peroxide (1.6 mg/mL in 0.06 mol/L Tris buffer, Sigma-Aldrich) for 15 min. Slides were counterstained with hematoxylin, mounted in Cytoseal XYL (Richard Allen Scientific), visualized with a Zeiss Axioskop 2 plus microscope, and photographed with a Zeiss AxioCam camera.

Caspase-3 staining. Sections were stained with rabbit anti–caspase-3 primary antibody (1:100, Dakocytomation)

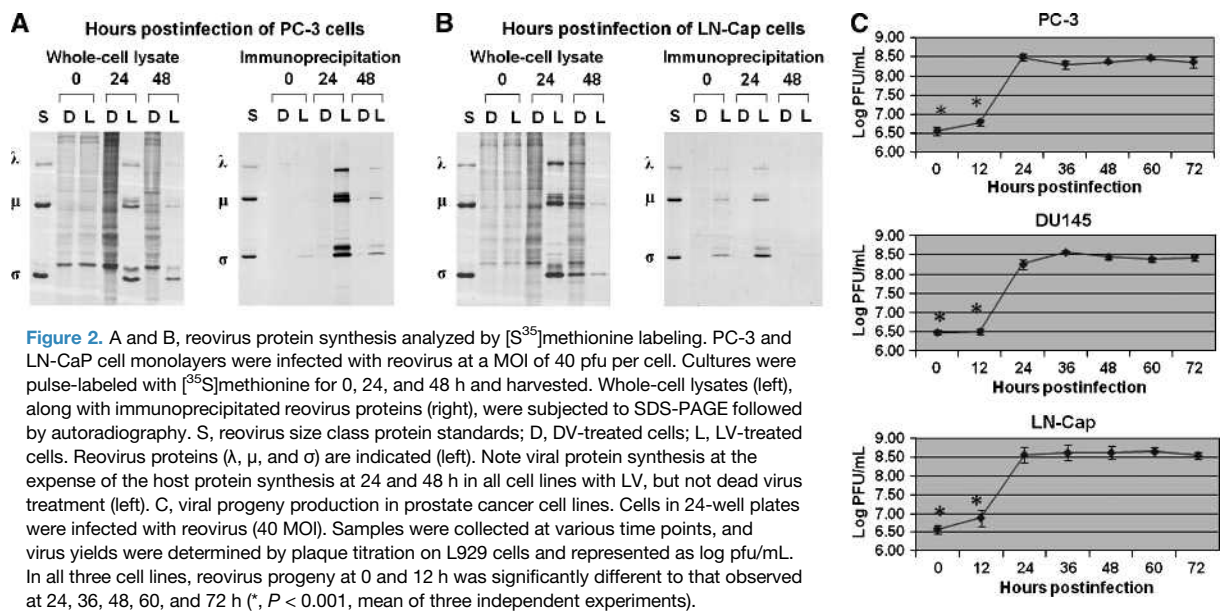

Figure 2. A and B, reovirus protein synthesis analyzed by [S^{35}]methionine labeling. PC-3 and LN-CaP cell monolayers were infected with reovirus at a MOI of 40 pfu per cell. Cultures were pulse-labeled with [^{35}S]methionine for 0, 24, and 48 h and harvested. Whole-cell lysates (left), along with immunoprecipitated reovirus proteins (right), were subjected to SDS-PAGE followed by autoradiography. S, reovirus size class protein standards; D, DV-treated cells; L, LV-treated cells. Reovirus proteins (λ, μ, and σ) are indicated (left). Note viral protein synthesis at the expense of the host protein synthesis at 24 and 48 h in all cell lines with LV, but not dead virus treatment (left). C, viral progeny production in prostate cancer cell lines. Cells in 24-well plates were infected with reovirus (40 MOI). Samples were collected at various time points, and virus yields were determined by plaque titration on L929 cells and represented as log pfu/mL. In all three cell lines, reovirus progeny at 0 and 12 h was significantly different to that observed at 24, 36, 48, 60, and 72 h (*, $P < 0.001$, mean of three independent experiments).

Published OnlineFirst March 9, 2010; DOI: 10.1158/0008-5472.CAN-09-2408

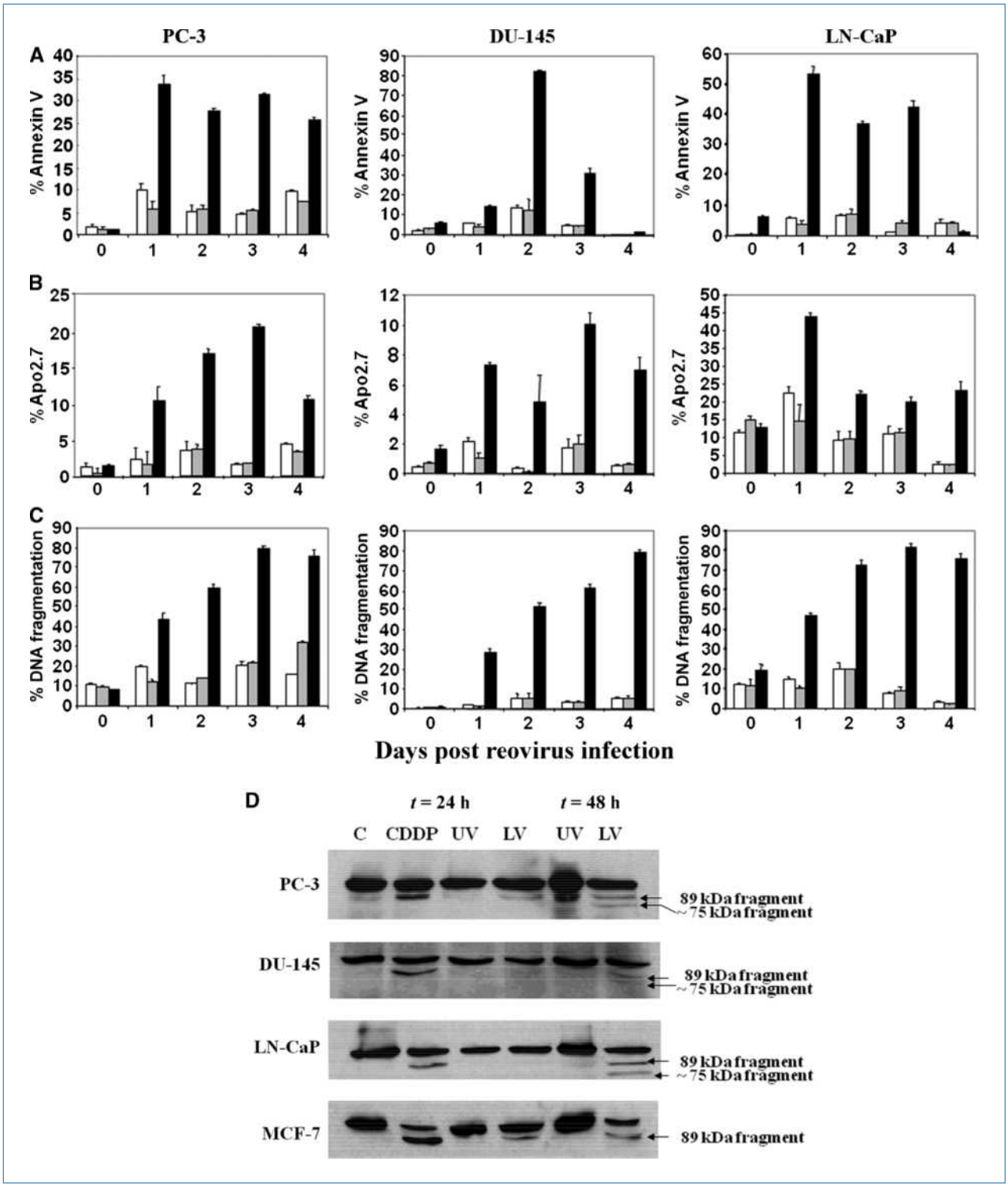

Figure 3. A-C, reovirus induced apoptosis of prostate cancer cell lines. PC-3, DU-145, and LN-CaP cells were harvested at various time points after being treated with no virus (white columns), DV (gray columns), or LV (black columns). Annexin V binding (A), Apo 2.7 expression (B), and DNA fragmentation analysis (C) were used as measures of apoptosis. Columns, percentage of mean (n = 3); bars, SEM. Note the significant increase in apoptotic markers in live virus–treated cells at days 1 to 4. D, Western blot analysis of reovirus-induced PARP cleavage. PC-3, DU-145, LN-CaP, and MCF-7 (breast cancer cell line) cells were treated either with cisplatinum (CDDP, 10 μg/mL) for 24 h or with DV (UV) or LV (MOI = 40 pfu) for 24 and 48 h. Whole-cell lysates were subjected to SDS-PAGE and probed with anti-PARP antibody. Note PARP cleavage in LV- or cisplatinum-treated cells and not in DV (UV)–treated cells. C, control cells.

Published OnlineFirst March 9, 2010; DOI: 10.1158/0008-5472.CAN-09-2408

and Envision + antirabbit HRP secondary antibody (Dakocytomation), counterstained with hematoxylin, visualized, and photographed.

Reovirus staining. Paraffin-embedded prostate tumor sections with no prior antigen retrieval were exposed to rabbit polyclonal antireovirus antibody (a kind gift from Dr. P. Forsyth, diluted 1:2,000) overnight at 4°C. They were next exposed to HRP-conjugated Envision + antirabbit secondary antibody (DAKO K1491) for 60 min. Further to counterstaining with hematoxylin (DAKO 3309), the slides were mounted in Cytoseal XYL, visualized, and photographed.

Statistical Analysis

Reovirus progeny production in prostate cell lines was analyzed as a one-way ANOVA to explore time effects on progeny production. All *in vivo* murine data for tumor size were analyzed for statistical significance by Wilcoxon rank sum test.

Results

In vitro Reovirus Oncolysis

As depicted in Fig. 1, PC-3, DU-145, and LN-CaP cell lines were found to be highly susceptible to reovirus-induced oncolysis. Marked cytopathic effects were detected in the LV-treated prostate cancer cells, but not in PrEC normal prostate epithelial cells (Fig. 1A). Immunofluorescence microscopy of infected cells stained with antireovirus antibody showed reovirus internalization and viral protein production by 24 hours (Fig. 1B). To determine that intracellular viral protein synthesis was occurring, SDS-PAGE analysis of cellular lysates from infected cells labeled with [^{35}S]methionine was undertaken. The prostate cell lines exhibited kinetics of viral protein synthesis by 24 hours (Fig. 2 A and B). In support of these results, increasing levels of pfu with prolonged incubation with reovirus were found in supernatants from LV-infected cultures, confirming that viral progeny are produced and released from host cells. Reovirus progeny release peaked by 24 hours in infected PC-3 and LN-CaP cultures and by 36 hours in infected DU-145 cultures (Fig. 2C).

The Role of Apoptosis in Reovirus-Mediated Oncolysis of Prostate Carcinoma Cell Lines

Previous studies have shown that reovirus-mediated cell death is preceded by several hallmark features of apoptosis, such as phosphatidyl serine flipping, membrane blebbing, loss of mitochondrial transmembrane potential, and DNA fragmentation (26–28). Figure 3A shows the early apoptotic event of phoshatidyl serine flipping detected by Annexin V binding at 24 hours in reovirus-infected PC-3 and LN-CaP cultures and by 48 hours in infected DU-145 cells. Indirect measure of the loss of mitochondrial transmembrane potential in reovirus-infected prostate cell lines was monitored through Apo 2.7 staining of the 38-kDa protein that is released from the mitochondria (Fig. 3B). DNA fragmentation assessed by a PI incorporation assay was significantly elevated in all three reovirus-infected cell lines, but not in dead virus–treated or uninfected cells (Fig. 3C). Finally, Western blot analysis of PARP cleavage performed in the three prostate cancer cell lines in conjunction with the breast cancer cell line (MCF-7) when treated with cisplatin (positive control) confirmed the appearance of an 89-kDa signature cleavage product at 24 hours. Whereas reovirus infection produced a distinctive pattern of PARP cleavage in the three prostate cancer cell lines consisting of both 89-kDa and 75-kDa fragments, it was of interest to note that the second PARP cleavage product (75 kDa)

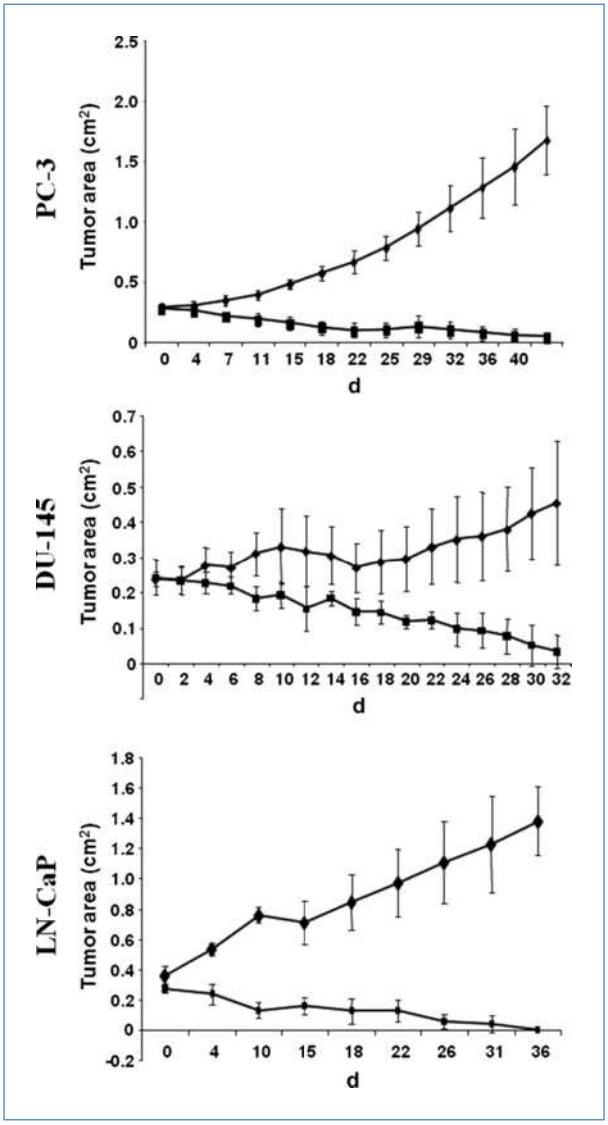

Figure 4. Effect of reovirus on prostate cancer cell line xenograft implants in SCID/NOD mice. Single hind flank implants of either PC-3, DU-145, or LN-CaP prostate cells were established in NOD/SCID mice. Tumors were injected with 1.0×10^7 pfu of LV at $t = 0$ d (■) or equivalent amount of DV (♦). Tumor growth was followed for 42, 32, and 36 d, respectively, at which time all control mice needed to be sacrificed owing to tumor burden. Points, mean tumor size; bars, SEM. PC-3 ($n = 8$), DU-145 ($n = 8$), and LN-CaP ($n = 5$) for each group. Note significant tumor reductions with LV treatments in contrast to DV treatments.

Published OnlineFirst March 9, 2010; DOI: 10.1158/0008-5472.CAN-09-2408

Table 1. Clinical study summary and reovirus virology and neutralizing antibodies

Patient no.	Stage (post prostatectomy)	Gleason score	PSA	Neutralizing antibody titer	Maximum toxicity grade	Pathologic response descriptors		
						Inflamation	Apoptsis	Necrosis
TB01	pT3aN_1	4 + 5	Baseline, 10.1	1:256	0	+	+	+
			Week 1	1:4096				
			Week 2	1:4096				
			Week 3, 10.6	1:4096				
TB02	pT3b	4 + 3	Baseline, 11.1	<1:8	0	0	+	0
			Week 1	1:1024				
			Week 2	1:4096				
			Week 3, 10.0	1:2048				
TB03	pT2b	3 + 4	Baseline, 3.2	1:8	0	0	0	0
			Week 1	1:1024				
			Week 2	1:2048				
			Week 3, 1.5	1:256				
TB04	pT3a	4 + 5	Baseline, 4.0	<1:8	0	+	+	0
			Week 1	1:32				
			Week 2	1:512				
			Week 3, 4.1	1:512				
TB05	pT3a	4 + 3	Baseline, 7.4	1:32	0	+	+	+
			Week 1	1:32				
			Week 2	1:1024				
			Week 3, 7.8	1:2048				
TB06	pT3a	3 + 5	Baseline, 14.0	<1:8	0	+	0	0
			Week 1	1:4096				
			Week 2	1:4096				
			Week 3, 15.6	1:2048				

was not seen in the reovirus-treated breast cancer cell line MCF-7 (caspase-3 deficient), thus suggesting differences between cell lines and/or histologies (Fig. 3D).

Effect of Reovirus on Human Prostate Cancer Tumors

In vivo

To study the effect of reovirus *in vivo*, a SCID/NOD xenograft s.c. hind flank murine model using the three prostate cell lines was examined for reovirus effect. All SCID/NOD mice implanted with DU-145 or PC-3 xenografts yielded tumors, whereas LN-CaP xenografts required Matrigel to propagate palpable tumors. Tumors were monitored to a size of ~0.25 cm^2 and then injected with 1×10^7 pfu of LV or an equivalent dose of DV as a negative control. Established xenograft tumors for all three cell lines showed a significant reduction in size after live virus treatment compared with treatment with dead virus after only one injection (Fig. 4). Although the response kinetics differed for all three cell lines tested, a significant difference in tumor progression compared with controls became evident for the LN-CaP xenografts by day 4, PC-3 xenografts by day 7, and DU-145 xenografts by day 8 (Wilcoxon rank sum test, $P = 0.0002$, $P = 0.0003$, and $P = 0.0079$, respectively). A significant difference in tumor size was also seen in mice treated with live virus (PC-3 at day 43, DU-145 at day 32, and LN-CaP day 36) compared with both day 0 and with control mice on the same date postinjection for each cell line (Wilcoxon rank sum test, $P = 0.0009$, $P = 0.0008$, and $P = 0.0083$, respectively).

Immunohistochemical analysis of the major organs of mice treated with live virus using a polyvalent antireovirus antisera revealed reovirus replication within the tumor mass, but not in other tissues analyzed (brain, kidney, lung, liver, and spleen), consistent with our previously shown nonhuman primate, canine, and rat data (29).

Effect of Reovirus in Prostate Cancer Patients

To assess the efficacy of reovirus in a clinical setting, a single intraprostatic injection of reovirus was performed in six patients with localized prostate carcinoma. This trial was built on the safety and efficacy data generated in a previously conducted intralesional phase I (REO 00.1) study (30). The study enrolled patients who had consented to a prostatectomy as their definitive cancer treatment after intratumoral injection of the reovirus 3 weeks before the planned surgery. Previous neoadjuvant antiandrogen therapy was an exclusion criteria. Patients underwent a transrectal ultrasound to identify a hypoechoic lesion that was then injected with 10^7 pfu of GMP grade reovirus (REOLYSIN). Stool, urine, and serum were tested for evidence of viral spread/shedding by viral culture and reverse transcription–PCR (RT-PCR). The reovirus

Published OnlineFirst March 9, 2010; DOI: 10.1158/0008-5472.CAN-09-2408

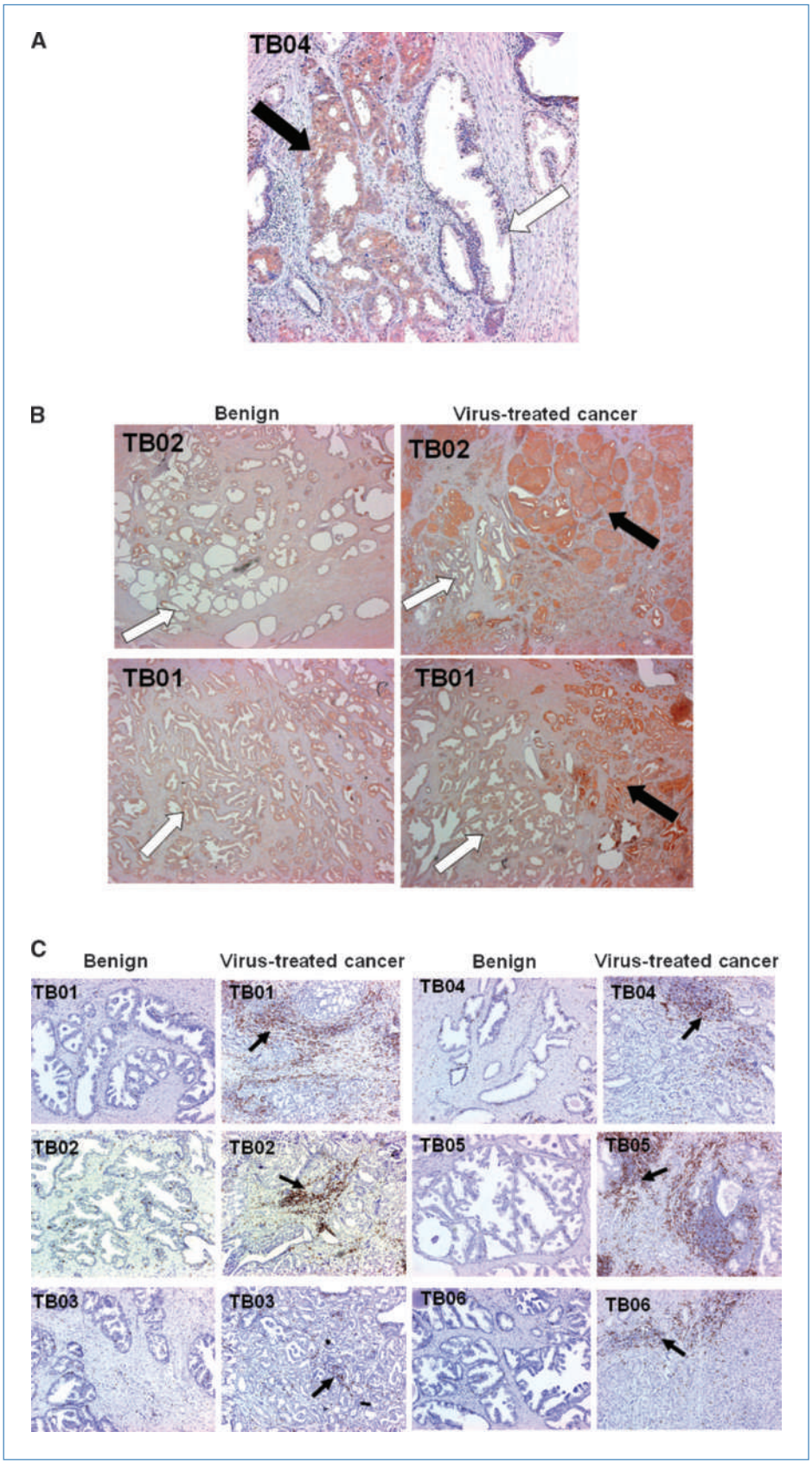

Figure 5. Immunohistochemical analysis of prostate sections from reovirus-infected patients. Prostate cancer patients were given a single injection of reovirus, and 2 wk after reovirus injection, prostate glands were surgically removed, paraffin embedded, sectioned, stained immunohistochemically, and analyzed by light microscopy. A, sections stained with antireovirus antibody (magnification, ×100). B, sections stained with caspase-3 antibody (magnification, ×25). A and B, black arrows point to cancerous tissue stained with antireovirus antibodies, whereas white arrows show benign tissue that is not invaded by reovirus. C, sections stained with CD8+ antibody (magnification, ×100). Arrows show lymphocyte infiltration in cancerous tissue that has been treated with reovirus. Significant T-cell infiltration was not detected in uninjected cancer areas of the prostate gland.

Published OnlineFirst March 9, 2010; DOI: 10.1158/0008-5472.CAN-09-2408

treatment was well tolerated, except for mild flu–like illness seen in four of six patients, which was self-limiting within 24 hours. No grade 3 or higher toxicities (NCI CTG version 4) were seen. Patient characteristics, toxicity, and markers of possible efficacy are given in Table 1. Interestingly, patients' PSA values did not fluctuate greatly from baseline despite of the significant peritumoral inflammation that occurred in several of the patients. Patients TB-02, TB-04, and TB-05 exhibited evidence of urine viral shedding in the urine in week 1 as detected by RT-PCR. Serum and stool were universally negative for both viral culture and RT-PCR viral products at all times tested (Table 1). As was seen with the original intralesional REO 00.1 phase I trial, a significant neutralizing antibody titer was detected within 1 week of the REOLYSIN injection (Table 1). This immune recognition likely limited viral spread to other areas of prostate cancer in those patients with multifocal disease, especially because only one injection was given. Interestingly, five of six patients that received reovirus treatment showed moderate to strong staining of reovirus proteins in cancer areas, whereas the adjacent benign areas and remote cancerous areas showed negative to weak staining of reovirus. This reiterated the fact that reovirus does not seem to infect noncancerous tissue, however unfortunately, also indicates that reovirus after a local injection likely does not spread to other areas of the prostate cancer in the same patient.

Pathologic evidence of necrosis and apoptotic bodies was accompanied by positive staining for reovirus protein and activated caspase-3 in the cancerous areas of pathologic specimens examined after prostatectomy (Fig. 5A and B). Immunohistochemical analysis also showed a substantial intratumoral CD8+ T-cell infiltration around the injected site, which may be suggestive of a possible immune strategy using reovirus in the future in the treatment of prostate cancer (Fig. 5C; ref. 31).

Discussion

This is the first study to provide evidence of efficacy for reovirus as a novel therapeutic modality for prostate cancer in both preclinical and clinical settings. A biological treatment modality, such as reovirus, has the potential to circumvent a number of toxicities associated with current treatments for localized prostate carcinoma, such as erectile dysfunction, bowel and bladder functional impairment, and other early and late effects. In addition, those patients in which radical radiotherapy or radical prostatectomy are contraindicated may well be candidates for reovirus therapy.

The current studies were performed to provide both preclinical and clinical data supporting the efficacy of reovirus as a therapeutic for prostate cancer. Significant tumor killing and cytopathic effects seen under *in vitro* conditions were confirmed further in the animal models wherein evidence of complete reovirus-induced tumor abrogation was seen with a single injection of reovirus in all three prostate cancer cell lines tested. Moreover, the small group of organ-confined patients in this study had minimal toxicity as a result of the treatment and only developed mild flu–like symptoms within the first 24 hours postinjection.

Interestingly, although all three prostate cancer cell lines tested were sensitive to reovirus, the LN-CaP (androgen independent) line was the most susceptible both in terms of absolute killing efficacy and the kinetics of this activity. This is suggestive that, although reovirus is oncolytic to androgen-sensitive cell lines, it may have important activity against hormone refractory prostate cancer. The finding that reovirus was not only able to trigger apoptosis in these cell lines but was also able to release viral progeny capable of killing other noninfected cancer cell argues that reovirus is able to set up an infectious lytic process that may be self-sustainable as long as there are sensitive cancer cells around that are able to sustain viral replication. This is likely the explanation for how a single reovirus injection was able to cure mice with viable growing tumors. This is in contrast to the multiple injections and higher doses required when a reovirus immunocompetent murine model has been used for other cancer histologies (29, 32). The neutralizing humoral immune response generated by reovirus exposure likely reduces the efficacy of a single injection and blunts the ability of progeny viruses to be generated, thus reducing the opportunity for a sustained infection in immunocompetent hosts. In all immunocompetent models tested thus far, this neutralizing immune response has been observed, including in the ongoing human trials with REOLYSIN[12] (33–35).

The histologic detection of CD8+ T-cell recruitment into reovirus-infected tumors is of interest. To date, although circulating tumor antigen–specific $CD8^+$ T lymphocytes are found in cancer patients, it is controversial whether T-cell infiltration into tumor correlates with tumor regression (36, 37). Moreover, it has also been shown that T cells will home to the peripheral margin of recurring mammary tumors without infiltrating the tumor proper and that these immune-effector cells are likely inhibited by the immunosuppressive nature of the tumor microenvironment (38). Promisingly, reovirus has been shown to induce secretion of proinflammatory factors mediating T-cell infiltration in a number of epithelial-derived cancer cell lines (39). It is plausible that a chemokine repertoire may be induced by reovirus infection in the patients of this study and that this provides a platform for overcoming inefficient T-cell homing.

These findings provide evidence for reovirus as a possible therapeutic for prostate cancer treatment. The SCID/NOD xenograft model confirmed the *in vitro* efficacy results; however, ongoing investigation is required using an immunocompetent model to address optimizing reovirus efficacy in the presence of intact humoral and cell-mediated immunity and circumvention of viral clearance. Nevertheless the role of REOLYSIN local/regional activity should not be discounted, as there is a significant preclinical and/or human clinical trial experience with REOLYSIN instillation for superficial bladder cancer (40) and as a radiation sensitizer for local regional control in head

[12] http://www.Oncolytics.Biotech.Inc

Published OnlineFirst March 9, 2010; DOI: 10.1158/0008-5472.CAN-09-2408

and neck cancers (35). The ultimate goal of these investigations is to provide the necessary preclinical data for a full phase I clinical trial in advanced prostate cancer.

Disclosure of Potential Conflicts of Interest

M. Coffey: employment and ownership interest, Oncolytics Biotech, Inc. The other authors disclosed no potential conflicts of interest.

Grant Support

Prostate Cancer Research Foundation of Canada, National Cancer Institute of Canada, Canadian Cancer Society and Oncolytics Biotech, Inc. (D.G. Morris).

The costs of publication of this article were defrayed in part by the payment of page charges. This article must therefore be hereby marked *advertisement* in accordance with 18 U.S.C. Section 1734 solely to indicate this fact.

Received 07/07/2009; revised 12/13/2009; accepted 01/11/2010; published OnlineFirst 03/09/2010.

References

1. Jemal A, Siegel R, Ward E, et al. Cancer statistics. CA Cancer J Clin 2008;58:71–96.
2. Parkin DM. Global cancer statistics in the year 2000. Lancet Oncol 2001;2:533–43.
3. Alain T, Hirasawa K, Pon KJ, et al. Reovirus therapy of lymphoid malignancies. Blood 2002;100:4146–53.
4. Hirasawa K, Nishikawa SG, Norman KL, Alain T, Kossakowska A, Lee PW. Oncolytic reovirus against ovarian and colon cancer. Cancer Res 2002;62:1696–701.
5. Norman KL, Coffey MC, Hirasawa K, et al. Reovirus oncolysis of human breast cancer. Hum Gene Ther 2002;13:641–52.
6. Himeno Y, Etoh T, Matsumoto T, Ohta M, Nishizono A, Kitano S. Efficacy of oncolytic reovirus against liver metastasis from pancreatic cancer in immunocompetent models. Int J Oncol 2005;27:901–6.
7. Wilcox ME, Yang W, Senger , et al. Reovirus as an oncolytic agent against experimental human malignant gliomas. J Natl Cancer Inst 2001;93:903–12.
8. Tyler KL. Reoviruses. In: Fields B, editor. Fields Virology. Philadelphia (PA): Lippincott-Raven; 1996, p. 1597–623.
9. Strong JE, Lee PW. The v-erbB oncogene confers enhanced cellular susceptibility to reovirus infection. J Virol 1996;70:612–6.
10. Strong JE, Coffey MC, Tang D, Sabinin P, Lee PW. The molecular basis of viral oncolysis: usurpation of the Ras signaling pathway by reovirus. EMBO J 1998;17:3351–62.
11. Coffey MC, Strong JE, Forsyth PA, Lee PW. Reovirus therapy of tumors with activated Ras pathway. Science 1998;282:1332–4.
12. Norman KL, Hirasawa K, Yang AD, Shields MA, Lee PW. Reovirus oncolysis: the Ras/RalGEF/p38 pathway dictates host cell permissiveness to reovirus infection. Proc Natl Acad Sci U S A 2004;101:11099–104.
13. Kinkade CW, Castillo-Martin M, Puzio-Kuter A, et al. Targeting AKT/mTOR and ERK MAPK signaling inhibits hormone-refractory prostate cancer in a preclinical mouse model. J Clin Invest 2008;18:3051–64.
14. Carracedo A, Ma L, Teruya-Feldstein J, et al. Inhibition of mTORC1 leads to MAPK pathway activation through a PI3K-dependent feedback loop in human cancer. J Clin Invest 2008;118:3065–74.
15. Roulston A, Marcellus RC, Branton PE. Viruses and apoptosis. Annu Rev Microbiol 1999;53:577–628.
16. Razvi ES, Welsh RM. Apoptosis in viral infections. Adv Virus Res 1995;45:1–60.
17. Rodgers SE, Barton ES, Oberhaus SM, et al. Reovirus-induced apoptosis of MDCK cells is not linked to viral yield and is blocked by Bcl-2. J Virol 1997;71:2540–6.
18. Oberhaus SM, Dermody TS, Tyler KL. Apoptosis and the cytopathic effects of reovirus. Curr Top Microbiol Immunol 1998;233:23–49.
19. Debiasi RL, Edelstein CL, Sherry B, Tyler KL. Calpain inhibition protects against virus-induced apoptotic myocardial injury. J Virol 2001;75:351–61.
20. Debiasi RL, Squier MK, Pike B, et al. Reovirus-induced apoptosis is preceded by increased cellular calpain activity and is blocked by calpain inhibitors. J Virol 1999;73:695–701.
21. Connolly JL, Rodgers SE, Clarke P, et al. Reovirus-induced apoptosis requires activation of transcription factor NF-κB. J Virol 2000;74:2981–9.
22. Clarke P, Meintzer SM, Moffitt LA, Tyler KL. Two distinct phases of virus-induced nuclear factor κB regulation enhance tumor necrosis factor-related apoptosis-inducing ligand-mediated apoptosis in virus-infected cells. J Biol Chem 2003;278:18092–100.
23. Clarke P, Meintzer SM, Gibson S, et al. Reovirus-induced apoptosis is mediated by TRAIL. J Virol 2000;74:8135–9.
24. Smith RE, Zweerink HJ, Joklik WK. Polypeptide components of virions, top component and cores of reovirus type 3. Virology 1969;39:791–810.
25. Cejkova S, Rocnova L, Potesil D, et al. Presence of heterozygous ATM deletion may not be critical in the primary response of chronic lymphocytic leukemia cells to fludarabine. Eur J Haematol 2009;82:133–42.
26. Jin D, Ojcius DM, Sun D, et al. Leptospira interrogans induces apoptosis in macrophages via caspase-8- and -3-dependent pathways. Infect Immun 2009;77:799–809.
27. Aubry JP, Blaecke A, Lecoanet-Henchoz S, et al. Annexin V used for measuring apoptosis in the early events of cellular cytotoxicity. Cytometry 1999;37:197–204.
28. Koester SK, Roth P, Mikulka WR, Schlossman SF, Zhang C, Bolton WE. Monitoring early cellular responses in apoptosis is aided by the mitochondrial membrane protein-specific monoclonal antibody APO2.7. Cytometry 1997;29:306–12.
29. Yang WQ, Lun X, Palmer CA, et al. Efficacy and safety evaluation of human reovirus type 3 in immunocompetent animals: racine and nonhuman primates. Clin Cancer Res 2004;10:8561–76.
30. Morris DG, Forsyth PA, Paterson AH, et al. A phase 1 clinical trial evalutating entralesional REOLYSIN (reovirus) in histologically confirmed malignancies. Proc ASCO 2002:24a.
31. Spurrell JC, Shi ZQ, Kim A, Morris DG. Reovirus as an Immunotherapeutic adjuvant. Canadian Prostate Cancer Research Foundation Annual Meeting. 2007, Abstr.
32. Hirasawa K, Nishikawa SG, Norman KL, et al. Systemic reovirus therapy of metastatic cancer in immune-competent mice. Cancer Res 2003;63:348–53.
33. White CL, Twigger KR, Vidal L, et al. Characterization of the adaptive and innate immune response to intravenous oncolytic reovirus (Dearing type 3) during a phase I clinical trial. Gene Ther 2008;15:911–920.
34. Vidal L, Twigger K, White CL, et al. Phase I trial of intratumoral administration of reovirus type 3 (REOLYSIN) in combination with radiation in patients with advanced malignancies. Clin Res 2008;13:Abstr.
35. Twigger K, Vidal L, White CL, et al. Enhanced *in vitro* and *in vivo* cytotoxicity of combined reovirus and radiotherapy. Clin Cancer Res 2008;14:912–23.
36. Douville RN, Su RC, Coombs KM, Simons FE, Hayglass KT. Reovirus serotypes elicit distinctive patterns of recall immunity in humans. J Virol 2008;82:7515–23.
37. Talmadge JE, Donkor M, Scholar E. Inflammatory cell infiltration of tumors: Jekyll or Hyde. Cancer Metastasis Rev 2007;26:373–400.
38. Yu P, Fu YX. Tumor-infiltrating T lymphocytes: friends or foes. Lab Invest 2006;86:231–245.
39. Hamamdzic D, Phillips-Dorsett T, Altman-Hamamdzic S, London SD, London L. Reovirus triggers cell type-specific proinflamatory responses dependent on the autocrine action of IFN-β. Am J Physiol Lung Cell Mol Physiol 2001;280:L18–29.
40. Kilani RT, Tamimi Y, Hanel EG, et al. Selective reovirus killing of bladder cancer in a co-culture spheroid model. Virus Res 2003;93:1–12.

AACR American Association for Cancer Research

Cancer Research

The Journal of Cancer Research (1916–1930) | The American Journal of Cancer (1931–1940)

Oncolytic Viral Therapy for Prostate Cancer: Efficacy of Reovirus as a Biological Therapeutic

Chandini M. Thirukkumaran, Michael J. Nodwell, Kensuke Hirasawa, et al.

Cancer Res Published OnlineFirst March 9, 2010.